Anna Zampetaki,[1] Peter Willeit,[1,2,3] Simon Burr,[1] Xiaoke Yin,[1] Sarah R. Langley,[1] Stefan Kiechl,[3] Ronald Klein,[4] Peter Rossing,[5] Nishi Chaturvedi,[6] and Manuel Mayr[1]

Angiogenic microRNAs Linked to Incidence and Progression of Diabetic Retinopathy in Type 1 Diabetes

Diabetes 2016;65:216–227 | DOI: 10.2337/db15-0389

Circulating microRNAs (miRNAs) have emerged as novel biomarkers of diabetes. The current study focuses on the role of circulating miRNAs in patients with type 1 diabetes and their association with diabetic retinopathy. A total of 29 miRNAs were quantified in serum samples (*n* = 300) using a nested case-control study design in two prospective cohorts of the DIabetic REtinopathy Candesartan Trial (DIRECT): PROTECT-1 and PREVENT-1. The PREVENT-1 trial included patients without retinopathy at baseline; the PROTECT-1 trial included patients with nonproliferative retinopathy at baseline. Two miRNAs previously implicated in angiogenesis, miR-27b and miR-320a, were associated with incidence and with progression of retinopathy: the odds ratio per SD higher miR-27b was 0.57 (95% CI 0.40, 0.82; *P* = 0.002) in PREVENT-1, 0.78 (0.57, 1.07; *P* = 0.124) in PROTECT-1, and 0.67 (0.50, 0.92; *P* = 0.012) combined. The respective odds ratios for higher miR-320a were 1.57 (1.07, 2.31; *P* = 0.020), 1.43 (1.05, 1.94; *P* = 0.021), and 1.48 (1.17, 1.88; *P* = 0.001). Proteomics analyses in endothelial cells returned the antiangiogenic protein thrombospondin-1 as a common target of both miRNAs. Our study identifies two angiogenic miRNAs, miR-320a and miR-27b, as potential biomarkers for diabetic retinopathy.

Recent studies have begun to unveil a powerful and unexpected role of microRNAs (miRNAs) in numerous forms of diseases, providing a unique opportunity to translate this knowledge into the clinical setting in the form of miRNA-based therapeutics and diagnostics (1,2). miRNAs are small noncoding RNAs with cell-type specific expression patterns that orchestrate biological networks by modulating gene expression. miRNAs form base pairs with their target messenger RNAs and mediate gene silencing, often regulating multiple proteins within the same biological pathways. Given their importance in angiogenesis, along with the technical feasibility in manipulating their function in vivo, vascular miRNAs have become central targets for therapeutic manipulation, including diabetes (3).

Additionally, miRNAs circulate in blood. We have previously performed the first systematic analysis of circulating miRNAs in a population-based study (the Bruneck Study) and identified distinct miRNA signatures associated with type 2 diabetes (4) and risk of myocardial infarction (5). We have also highlighted their platelet origin (6) and applied concepts of network topology to explore their biomarker potential (7). Exciting opportunities exist to pursue miRNAs as novel biomarkers for risk estimation and patient stratification (8).

The current study addresses the role of circulating miRNAs in patients with type 1 diabetes (T1D) and their association with microvascular complications, in particular, diabetic retinopathy. Our aims were threefold: first, to evaluate whether miRNA profiles are independently associated with retinopathy development and progression in diabetes; second, to quantify the incremental discriminatory power of miRNAs over and above traditional risk markers; and third, to conduct experiments

[1]King's British Heart Foundation Centre of Research Excellence, King's College London, London, U.K.
[2]Department of Public Health and Primary Care, University of Cambridge, Cambridge, U.K.
[3]Department of Neurology, Medical University of Innsbruck, Innsbruck, Austria
[4]Department of Ophthalmology and Visual Sciences, University of Wisconsin–Madison, Madison, WI
[5]Steno Diabetes Centre, University of Copenhagen, Copenhagen, Denmark
[6]Institute of Cardiovascular Science, University College London, London, U.K.
Corresponding author: Nishi Chaturvedi, n.chaturvedi@ucl.ac.uk., or Manuel Mayr, manuel.mayr@kcl.ac.uk.

Received 21 March 2015 and accepted 16 September 2015.
This article contains Supplementary Data online at http://diabetes.diabetesjournals.org/lookup/suppl/doi:10.2337/db15-0389/-/DC1.

A.Z. and P.W. share first authorship.

N.C. and M.M. share senior authorship.

See accompanying article, p. 22.

using endothelial cells (ECs) and proteomics profiling to provide mechanistic insight.

RESEARCH DESIGN AND METHODS

Patient Sample

The DIabetic REtinopathy Candesartan Trials (DIRECT) trials have previously been described in detail (9). In brief, two randomized, double-blind, parallel-design, and placebo-controlled trials (PREVENT-1 and PROTECT-1) were conducted in 309 centers worldwide. Both trials assigned patients with normotensive, normoalbuminuric T1D to either candesartan 16 mg once a day or placebo. Exclusion criteria were eye conditions that precluded capture of gradable retinal photographs (i.e., open-angle glaucoma, dense cataract obscuring retinal view), stenotic valvular disease, previous history of heart attack or stroke, pregnancy, lactation, or renal impairment (serum creatinine $\geq$110 μmol/L for women, $\geq$130 μmol/L for men). The PREVENT-1 trial included patients without retinopathy at baseline (defined as Early Treatment Diabetic Retinopathy Study [ETDRS] scale level 10/10); the PROTECT-1 trial included patients with nonproliferative retinopathy at baseline (defined as ETDRS scale between 20/10 and 47/47). For the current study, we used a "nested" case-control approach. Incident case subjects were defined as patients who progressed three steps or more on the ETDRS scale over the course of the study. Case subjects were stratum matched with control subjects on sex, HbA_{1c} categories, and categories of diabetes duration (plus an ETDRS summary score in PROTECT-1). These were randomly selected from participants whose ETDRS scale did not progress and who remained free of intermittent microalbuminuria to the end of the study period. Numbers selected for analysis were 70 case and 70 control subjects in PREVENT-1 and 93 case and 93 control subjects in PROTECT-1. Analysis of miRNAs could not be performed on all serum samples. Thus, the number of case and control subjects in the present analysis was 62 and 64 in PREVENT-1 and 81 and 93 in PROTECT-1 (n = 300).

miRNA Measurements

Total RNA from 200 μL of serum samples was prepared using the miRNeasy kit (Qiagen) as previously described (4). A fixed volume of 3 μL of the 25 μL RNA eluate was used as input for RT reactions using Megaplex Primer Pools (Human Pools A, version 2.1, Life Technologies). RT reaction products were further amplified using the Megaplex PreAmp Primers (Primers A, version 2.1). TaqMan miRNA assays were used to assess the expression of individual miRNAs. Diluted preamplification product (0.5 μL) was combined with 0.25 μL TaqMan miRNA Assay (20×) (Life Technologies) and 2.5 μL TaqMan Universal PCR Master Mix No AmpErase UNG (2×) to a final volume of 5 μL. Quantitative PCR was performed on a Life Technologies ViiA 7 thermocycler at 95°C for 10 min, followed by 40 cycles of 95°C for 15 s and 60°C for 1 min. All samples were run in duplicates. Relative quantification was performed using the DataAssist, version 3.01 (Life Technologies). For normalization purposes, the average of all miRNA targets displaying C_t <32 cycles or an exogenous miRNA (*cel*-miR-39) spiked in during RNA extraction was applied as previously described (5).

Transfection

Human umbilical vein endothelial cells (HUVECs) were cultured as described previously (10) and seeded at 60–70% confluency on the day before transfection. Cells were washed in serum-free DMEM and replaced with M199 containing ECs supplement without antibiotics or serum. Human retinal microvascular ECs (HRECs) (obtained from Cell Systems Corporation [CSC], Kirkland, WA) were seeded on CSC attachment factor (cat. no. 4Z0-210) and cultured in CSC complete media (cat. no. 4Z0-500). Prior to transfection, HRECs were washed with CSC Serum Free Medium without antibiotics (cat. no. SF-4Z0-500). miRNA mimics or nontargeting mimic control were transfected at a final concentration of 50 nmol/L using Lipofectamine RNAiMAX (Invitrogen) according to the manufacturer's recommendations (11).

Proteomic Profiling of the Endothelial Secretome

HUVECs were carefully washed in serum-free medium and then incubated twice in fresh serum-free M199 for 30 min. Cells were stimulated in phorbol 12-myristate 13-acetate (PMA) (50 nmol/L) containing M199 medium for 45 min and analyzed by mass spectrometry as previously described (10). The conditioned medium was collected, centrifuged at 1000 rpm for 5 min, and concentrated using Amicon Ultra-15 Centrifugal Filter Unit with Ultracel-3 membrane (3 KDa) (Millipore) to 135 μL. Then, 0.5 mol/L Tris; 1% SDS, pH 8.8 (15 μL); and 100 mmol/L dithiothreitol reducing agent (7.8 μL) were added under agitation for 1 h at 55°C, followed by incubation with 500 mmol/L iodoacetamide (8.3 μL) for 1 h before precipitation with cold acetone (−20°C) overnight at −20°C. Samples were centrifuged (14,000 rpm for 10 min), the supernatant was discarded, and the protein pellet was left to air-dry. Pellets were resuspended in 0.1 mol/L, pH 8.5, triethylammonium bicarbonate (100 μL) and incubated at 37°C under agitation for 30 min. Proteins were digested in 0.4 μg/μL trypsin (1 μL) overnight at 37°C. The reaction was stopped by addition of 10% formic acid (50 μL). Peptide samples were purified using C18 spin columns (Thermo Scientific). The eluate was kept at −80°C before freeze drying (Christ Alpha 1-2 LD Freeze Dryer) under vacuum at −55°C. The samples were resuspended in 2% acetonitrile and 0.1% formic acid (20 μL) and analyzed by reverse-phase nanoflow high-performance liquid chromatography (3 μmol/L, 100 Å, 50 cm × 75 μm inner diameter column, Acclaim PepMap C18, Thermo Scientific) interfaced with a Q Exactive Plus Orbitrap mass spectrometer (Thermo Scientific). Each sample was separated at a flow rate of 0.3 μL/min over 4 h as follows: 0–10 min/2–10% of 80% acetonitrile and 0.1% formic acid in ddH_2O (B), 10–200 min/10–30%B, 200–210 min/30–40%B, 210–220 min/99%B, and 220–240 min/2%B. Samples were subject to a full mass spectrometry scan over a

range from 350 to 1,600 m/z, whereby the 15 most abundant peaks were selected for tandem mass spectrometry and fragmented by higher-energy collisional dissociation.

Database Search

Raw data were analyzed by Mascot and Sequest HT algorithms (Proteome Discoverer 1.4) to identify proteins against Swiss-Prot protein database (version 201401) with taxonomy set to all entries, precursor mass tolerance to 10 ppm, fragment mass tolerance to 20 mmu, oxidation of methionine as a variable modification and carbamidomethylation of cysteine as a static modification, and a maximum of two missed cleavage sites permitted. Search results were loaded onto Scaffold software (version 4.3), where a protein probability >99%, a peptide probability >95%, and a minimum number of two peptides per protein were applied as filters to generate the list of identified proteins.

Luciferase Reporter Assays

The 3′-untranslated region of the human neuropilin 1 (NRP1) and semaphorin 6A (SEMA6A) harboring a putative binding site for miR-320a and miR-27b, respectively, was cloned into the XhoI and PmeI linkers of the dual-luciferase reporter vector psiCHECK-2 (Promega). The following primer sets were used: NRP, F: TTCAATGAGTATGGCCGACA; NRP, R: GGATTTCGCTCAGTTTCC; SEMA6A, F: CGCACAGAGGT GAACAGAAA; and SEMA6A, R: GCCCAACATGGCATT TATCT.

The reporter constructs (100 ng) were transfected together with their respective miRNA mimics (50 nmol/L) or mimic control in triplicate into HUVECs, previously plated (post 12 h) in 6-well plates using Lipofectamine RNAiMAX (Invitrogen) as described above. After 48 h, cells were harvested in 200 μL Glo Lysis Buffer (Promega) and the activities of both Renilla and firefly were measured. Each lysate (30 μL) was analyzed using Dual-Glo Luciferase reagents (Promega). Renilla luciferase activity was normalized to constitutive firefly luciferase activity for each well.

ELISAs

Thrombospondin-1 (TSP-1) levels in the conditioned media were determined using the Human Thrombospondin-1 Quantikine ELISA kit (Bio-Techne) according to the manufacturer's instruction.

Statistical Analysis

miRNA values were log transformed for analysis. Pairwise correlations between miRNAs and other markers were assessed using Pearson correlation coefficients in a pooled data set of 145 control subjects and plotted with the R package "corrplot" using hierarchical clustering and the single linkage method. We analyzed the association of miRNAs with incident retinopathy in two steps. First, to identify the miRNA subset with the highest prognostic ability for future retinopathy, we used a L_1-penalized logistic regression technique. This method helps prevent overfitting of collinear and high-dimensional data and implements the "least absolute shrinkage and selection operator" (LASSO) algorithm, shrinking regression coefficients toward zero relative to the maximum likelihood estimates. The amount of shrinkage is determined by the tuning parameter λ_1, which is progressively increased up to the value that shrinks all regression coefficients to zero. We estimated the optimal tuning parameter λ_1 as the median of 10,000 fivefold likelihood cross-validations. Plots of β-coefficients (*y*-axis) versus λ_1 (*x*-axis) were generated using the R package "penalized." Sensitivity analyses were conducted that *1*) standardized miRNA concentrations to a global C_t average (instead of to *cel*-miR-39) and *2*) excluded participants from analysis with diabetic nephropathy or microalbuminuria. Because the LASSO method allows assessment of relevance and robustness of individual explanatory variables but produces biased estimates of β-coefficients, we fitted, as a second step, "traditional" logistic regression models for identified miRNAs. Analyses were adjusted for age, sex, and diastolic blood pressure and conducted separately for the two trials. A pooled estimate of association was calculated with random-effects meta-analysis. Between-study heterogeneity was assessed by the I^2 statistic (12). Regarding the experimental studies, results are presented as the mean ± SEM. For results from transfected ECs, paired or unpaired Student *t* test, one-way ANOVA with Dunnett or Tukey post hoc analysis, and two-way ANOVAs were performed using GraphPad Prism 5 software. With allowance for loss due to missing miRNA measurement, our sample size allowed us to detect a difference in retinopathy incidence and in progression in association with a standardized difference of 0.4 and 0.5, respectively, for any given miRNA signal with 80% power and 5% significance. Analysis was performed using R 3.1.3 statistical software (13) and Stata/MP, version 12/1, with two-sided tests and $P < 0.05$.

RESULTS

Associations of miRNAs With Incidence and Progression of Retinopathy in the DIRECT Trials

From the PREVENT-1 and PROTECT-1 trials of a total of 3,326 participants with T1D, we selected 62 patients with incident diabetes retinopathy, 93 patients with progressive diabetes retinopathy, and 145 matched control subjects. Supplementary Table 1 compares clinical characteristics of participants selected for the nested case-control analysis and those not selected. A panel of 29 miRNAs, of which some were previously shown to be associated with type 2 diabetes (4) and cardiovascular disease (5), was measured in serum and values were standardized to an exogenous spike-in normalization control, *cel*-miR-39. Baseline characteristics of study participants are summarized in Table 1. The ratio of males to females and mean diabetes duration were similar in case and control subjects within each trial, as anticipated owing to matching. Mean HbA_{1c}, however, was a little higher in control subjects, reflecting the fact that case and control subjects were stratum rather than individually matched by HbA_{1c}. Differences in age and

Table 1—Baseline characteristics of the study populations

	PREVENT-1			PROTECT-1		
	Case subjects	Control subjects	P‡	Case subjects	Control subjects	P‡
n	62	64		93	81	
Age at randomization, years	31.1 (8.1)	27.7 (8.1)	0.02	31.5 (9.1)	31 (8.5)	0.7
Male sex, *n* (%)	33 (53)	37 (58)	0.7	58 (62)	42 (52)	0.2
Duration of diabetes, years	7.3 (3.8)	7.3 (3.6)	1.0	10.9 (4.0)	10.6 (4.0)	0.7
Systolic blood pressure, mmHg	116 (9.1)	119 (9.6)	0.04	117 (10.8)	118 (8.9)	0.7
Diastolic blood pressure, mmHg	72 (7.7)	73 (6.5)	0.3	72.7 (7.0)	75 (6.4)	0.02
HbA_{1c}, %	8.9 (1.5)	9.2 (1.8)	0.4	8.9 (1.2)	9.4 (1.5)	0.05
UAER, μg/min	4.8 [3.3, 6.5]	4.3 [3.5, 6.0]	0.4	5.0 [3.0, 6.5]	5.0 [3.5, 9.5]	0.2
WHR all	0.81 (0.07)	0.83 (0.09)	0.08	0.85 (0.08)	0.82 (0.08)	0.1
WHR men	0.84 (0.07)	0.88 (0.09)	0.03	0.88 (0.07)	0.88 (0.07)	0.4
WHR women	0.77 (0.05)	0.77 (0.05)	0.9	0.78 (0.07)	0.77 (0.07)	0.5
Creatinine, μmol/L	89.7 (13)	90.0 (14)	0.9	88.1 (13.8)	86.7 (14.1)	0.6
GFR, mL/min/1.73 m^{2*}	88 [75, 107]	90 [79, 105]	0.8	92 [77, 107]	94 [80, 104]	0.8
GFR, mL/min/1.73 m^{2**}	83 [71 ,96]	83 [73, 98]	0.8	86 [73, 100]	88 [75, 96]	0.6
HDL cholesterol, mmol/L	1.7 (0.3)	1.7 (0.4)	0.6	1.7 (0.4)	1.8 (0.4)	0.07
Total cholesterol, mmol/L	4.7 (1.1)	4.9 (0.9)	0.5	5.1 (1.1)	4.9 (0.8)	0.2
Insulin dose, units/kg/day	0.77 (0.21)	0.69 (0.24)	0.07	0.81 (0.30)	0.71 (0.20)	0.01
eGDR, mg/kg/min***	9.2 (1.3)	9.0 (1.4)	0.4	8.6 (1.3)	9.1 (1.3)	0.02
Never smoker	34 (55)	47 (73)		50 (54)	54 (67)	
Ex-smoker	7 (11)	2 (3)		5 (5)	8 (10)	
Current smoker	21 (34)	15 (24)	0.02	38 (41)	19 (23)	0.08

Data are mean (SD) or median [interquartile range] unless otherwise indicated. eGDR, estimated glucose disposal rate; GFR, glomerular filtration rate; UAER, urinary albumin excretion rate; WHR, waist-to-hip ratio. ‡*P* values were calculated using Fisher exact tests for categorical variables, two-group *t* tests for continuous normally distributed variables, or Wilcoxon rank sum tests for continuous left-skewed variables. *Chronic Kidney Disease Epidemiology Collaboration (CKD-EPI) (44). **4-variable Modification of Diet in Renal Disease (MDRD) (45). ***Estimated glucose disposal rate as previously described (46).

blood pressure levels were also observed in the two study populations. The complex correlation patterns of serum miRNAs and baseline characteristics are depicted in Fig. 1. miRNAs emerged to be highly correlated with each other but largely independent from other characteristics such as age, duration of diabetes, blood pressure, and HbA_{1c}.

We conducted penalized logistic regression analyses adjusted for age, sex, and diastolic blood pressure to identify and evaluate the association of miRNAs with incidence and progression of diabetic retinopathy (Fig. 2 and Supplementary Fig. 1). The descriptive tables in Fig. 2 show the direction of association and the percentage of cross-validated models that included the respective miRNA. The following miRNAs were identified in descending order of importance: miR-27b, miR-320a, miR-454, and miR-28-3p in PREVENT-1 and miR-320a, miR-122, miR-221, and miR-27b in PROTECT-1. Generally, these miRNAs were more commonly selected for inclusion in cross-validated models for incidence than for progression of diabetic retinopathy (>90% vs. >10%). Results for all 29 individual miRNAs are provided in Supplementary Fig. 2 but should be interpreted with caution in light of multiple testing and type 1 error.

Since combinations of miRNAs can be superior to individual miRNAs (4,5,7), we then performed "traditional" logistic regression for the two miRNAs most consistently associated with incidence and progression of diabetic retinopathy: miR-27b and miR-320a. Figure 3 shows estimates of associations for miR-27b and miR-320a adjusted for each other, age, sex, and diastolic blood pressure. The odds ratio per SD higher miR-27b was 0.57 (95% CI 0.40, 0.82; P = 0.002) in PREVENT-1, 0.78 (0.57, 1.07; P = 0.124) in PROTECT-1, and 0.67 (0.50, 0.92; P = 0.012) combined. The respective odds ratios for higher miR-320a were 1.57 (1.07, 2.31; P = 0.020), 1.43 (1.05, 1.94; P = 0.021), and 1.48 (1.17, 1.88; P = 0.001). Qualitatively similar results were observed in analyses that *1*) standardized miRNA levels to a C_t average of all miRNAs (instead of standardization to spiked-in *cel*-miR-39) (Supplementary Fig. 3); *2*) excluded cases with incident microalbuminuria (Supplementary Fig. 3); *3*) used different levels of adjustment (unadjusted) or adjusted for age, sex, and systolic blood pressure or HbA_{1c}); or *4*) omitted outliers of the miRNA distributions. Supplementary Fig. 4 summarizes raw values of miR-27b and miR-320a for case and control subjects. Addition of information on

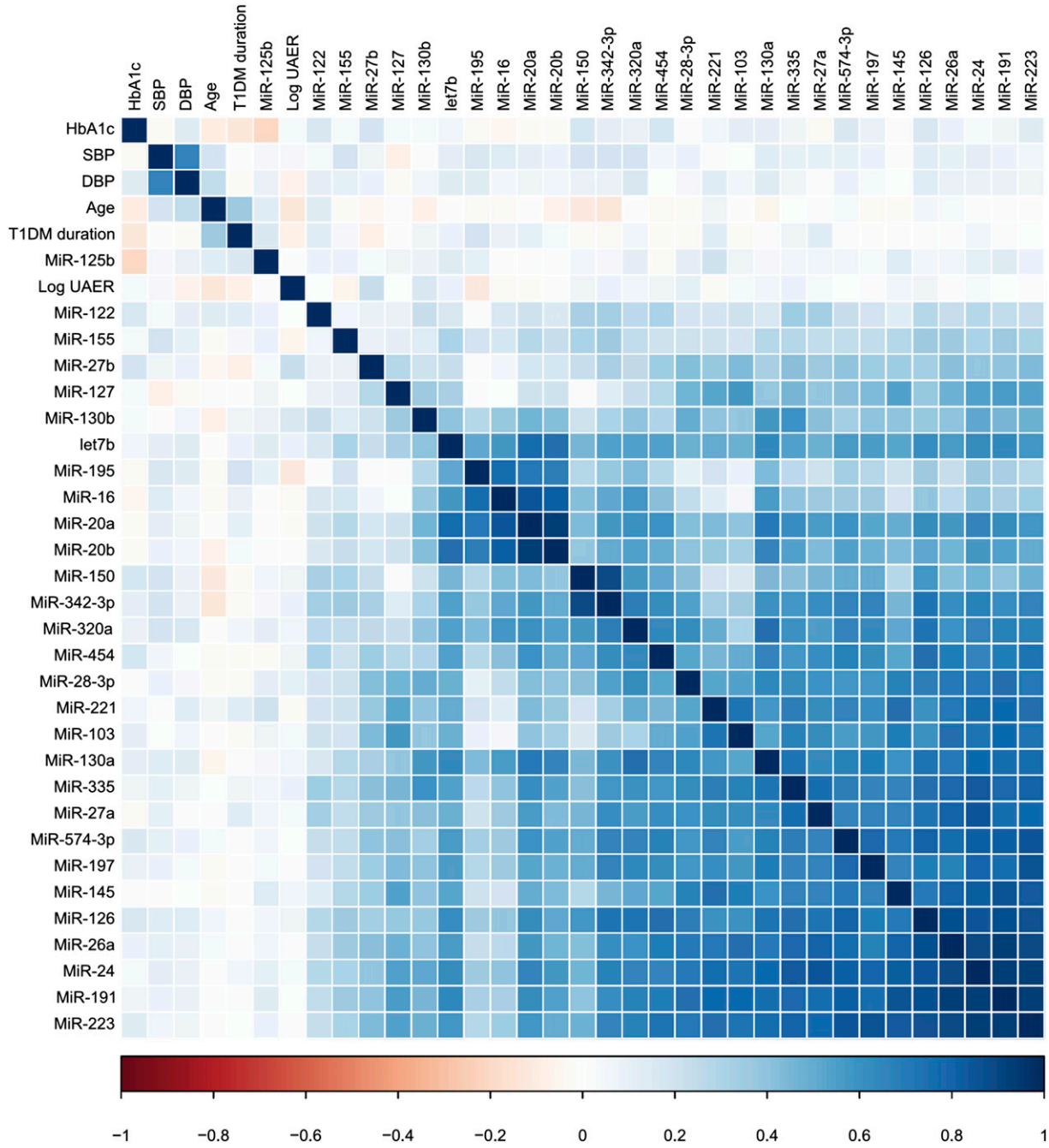

Figure 1—Pairwise Pearson correlation coefficients of serum miRNA concentrations and other markers. DBP, diastolic blood pressure; SBP, systolic blood pressure; T1DM, type 1 diabetes mellitus; UAER, urinary albumin excretion rate.

miR-27b and miR-320a to a model of a panel of variables associated with disease risk (i.e., age, sex, duration of diabetes, diastolic blood pressure, and level of HbA_{1c}) improved the area under the receiver operating curve by 0.087 for PREVENT-1 (P = 0.027) and by 0.034 for PROTECT-1 (P = 0.214) (Supplementary Fig. 5).

Expression of miRNAs in ECs

A PCR comparison was conducted to compare the endogenous expression of miR-27b and miR-320a to abundant endothelial miRNAs miR-126 and miR-126* (or miR-126-3p and miR-126-5p, respectively). There was no major difference in the endogenous miRNA expression of miR-27b, miR-320a, miR-126-3p, and miR-126-5p between four different types of ECs: human saphenous vein ECs, human aortic ECs, HRECs, and HUVECs (Supplementary Table 2). Notably, miR-320a was consistently more abundant in ECs than miR-27b. Next, mimics for miR-27b and miR-320a were cotransfected with luciferase reporter constructs containing putative binding site of two confirmed target proteins for miR-27b

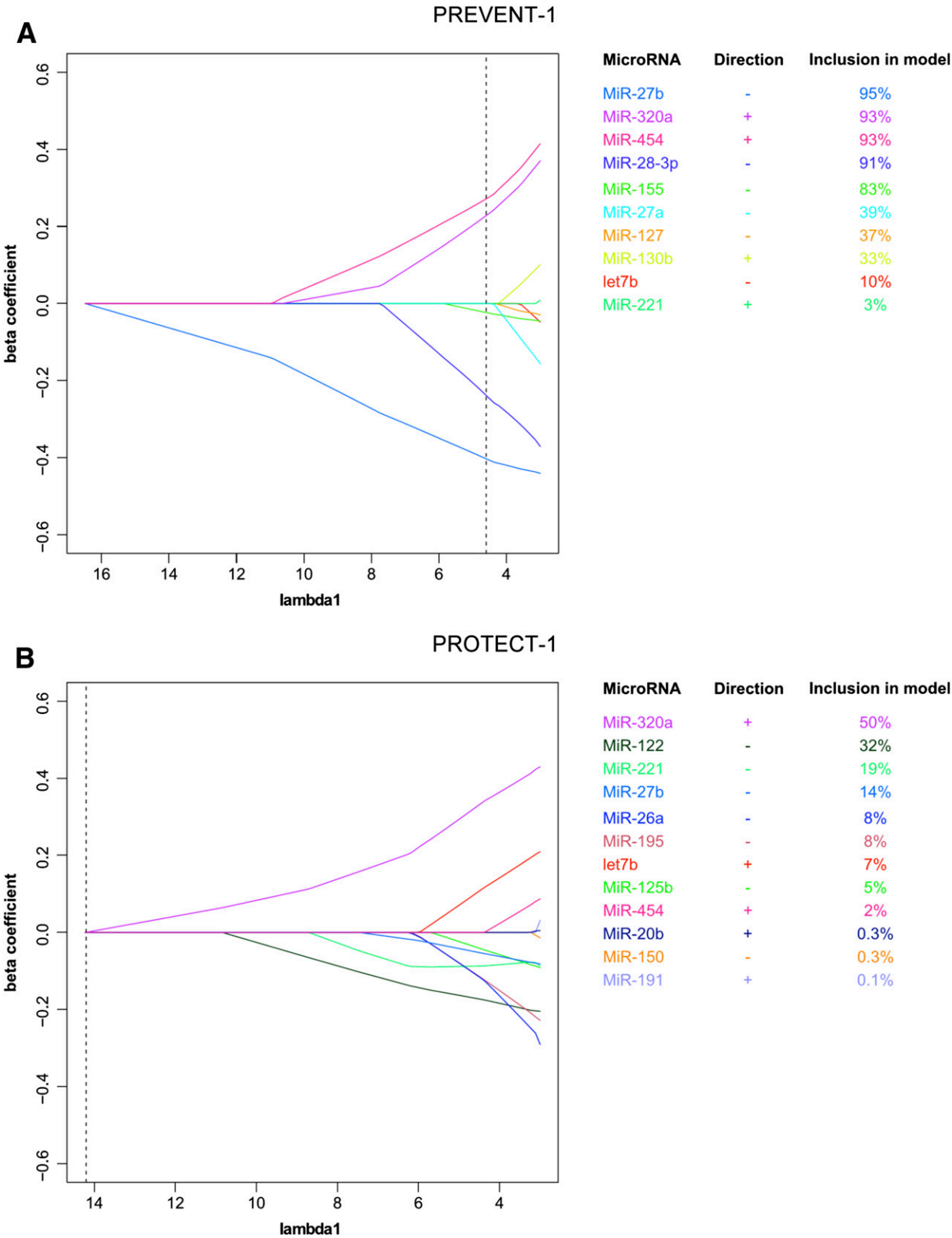

Figure 2—Penalized logistic regression analysis of the associations of 29 serum miRNA concentrations with diabetic retinopathy. Association with incident diabetic retinopathy in PREVENT-1 (*A*). Association with progression of diabetic retinopathy in PROTECT-1 (*B*). Models included age, sex, and diastolic blood pressure as unpenalized covariates. The graph shows β-coefficients for different levels of penalization (λ_1, estimated in 100 steps) and is truncated at a λ_1 of 3; hence, not all measured miRNAs are plotted. The black dashed line indicates the optimal tuning parameter λ_1 evaluated using 10,000 fivefold likelihood cross-validations. The descriptive table shows the direction of association and the percentage of cross-validated models that included the respective miRNA.

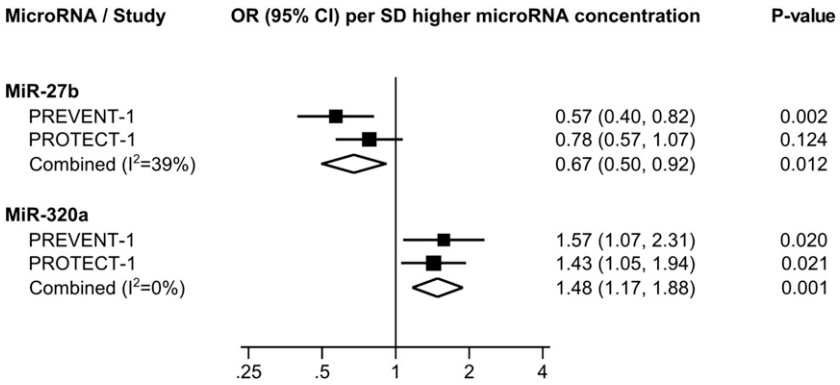

Figure 3—Standard logistic regression analysis and meta-analysis of the association of miR-27b and miR-320a with diabetic retinopathy and TSP-1 as common target in ECs. Association of miR-27b and miR-320a with diabetic retinopathy in PREVENT-1, PROTECT-1, and both studies combined. Associations of miR-27b and miR-320a with diabetic retinopathy were adjusted for each other plus age, sex, and diastolic blood pressure. SDs were defined in control subjects. Study-specific results were combined using random-effects meta-analysis. OR, odds ratio.

and miR-320a: SEMA6A and NRP1, respectively. SEMA6A is a negative regulator of mitogen-activated protein kinase signaling, known to increase transcription of angiogenic effector genes (14). NRP1 is a coreceptor for vascular endothelial growth factor (VEGF) and SEMA, promoting EC proliferation and microvessel density (15). Forty-eight hours after transfection, luciferase activity was found to be decreased by ~30% and 40% in SEMA6A and NRP1, respectively (Fig. 4*A* and *B*). Thereby, the functionality of miRNA mimics was confirmed through silencing expression of known targets.

Proteomics for miRNA Target Identification

We have demonstrated recently that direct and indirect targets can be identified in a broader proteomics screen,

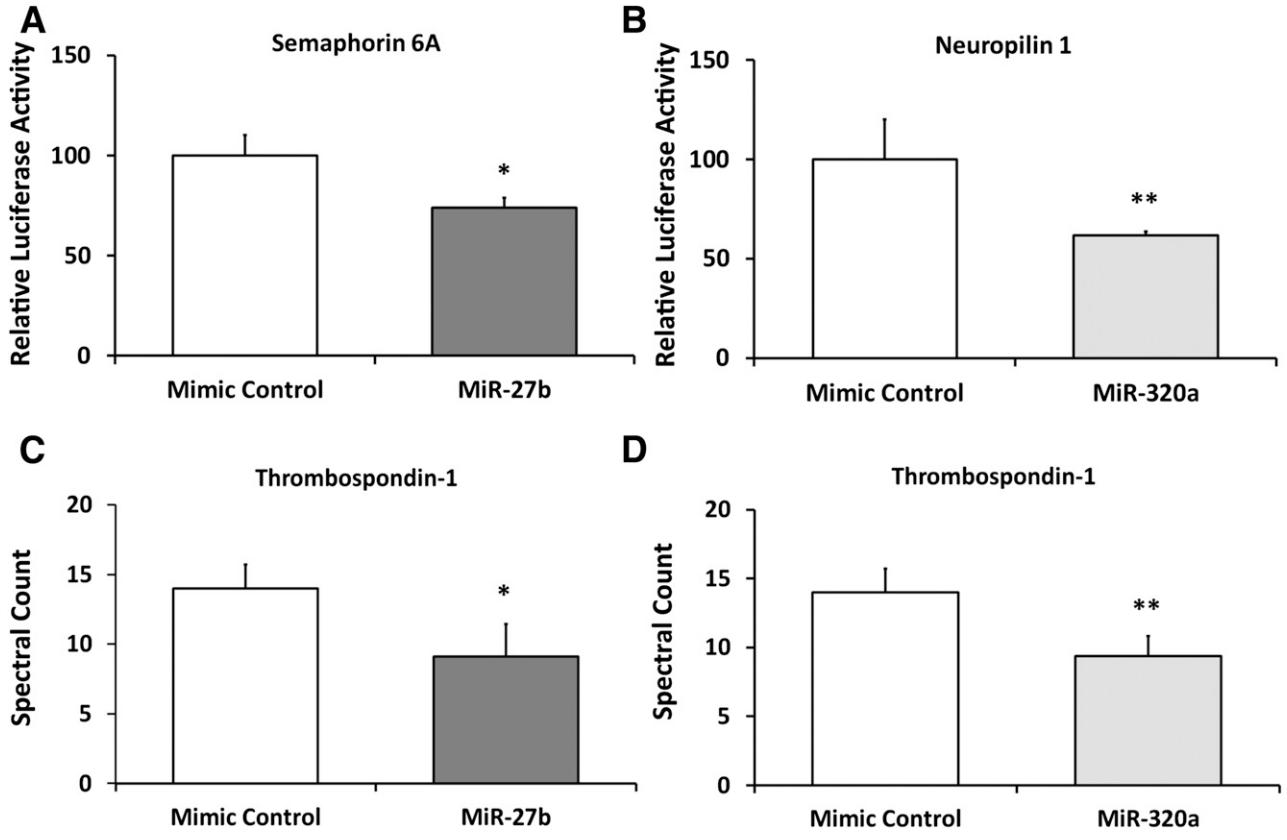

Figure 4—Proteomics for miRNA target identification. Luciferase reporter assays to confirm functional miRNA mimics. Suppression of SEMA6A (*A*), a known target of miR-27b, and NRP1 (*B*), a target of miR-320a. Spectral counts of TSP-1 as quantified by mass spectrometry in the secretome of ECs transfected with miR-27b (*C*) and miR-320a (*D*) compared with mimic controls. Error bars represent SEM. *$P < 0.05$ in three independent experiments, **$P < 0.01$.

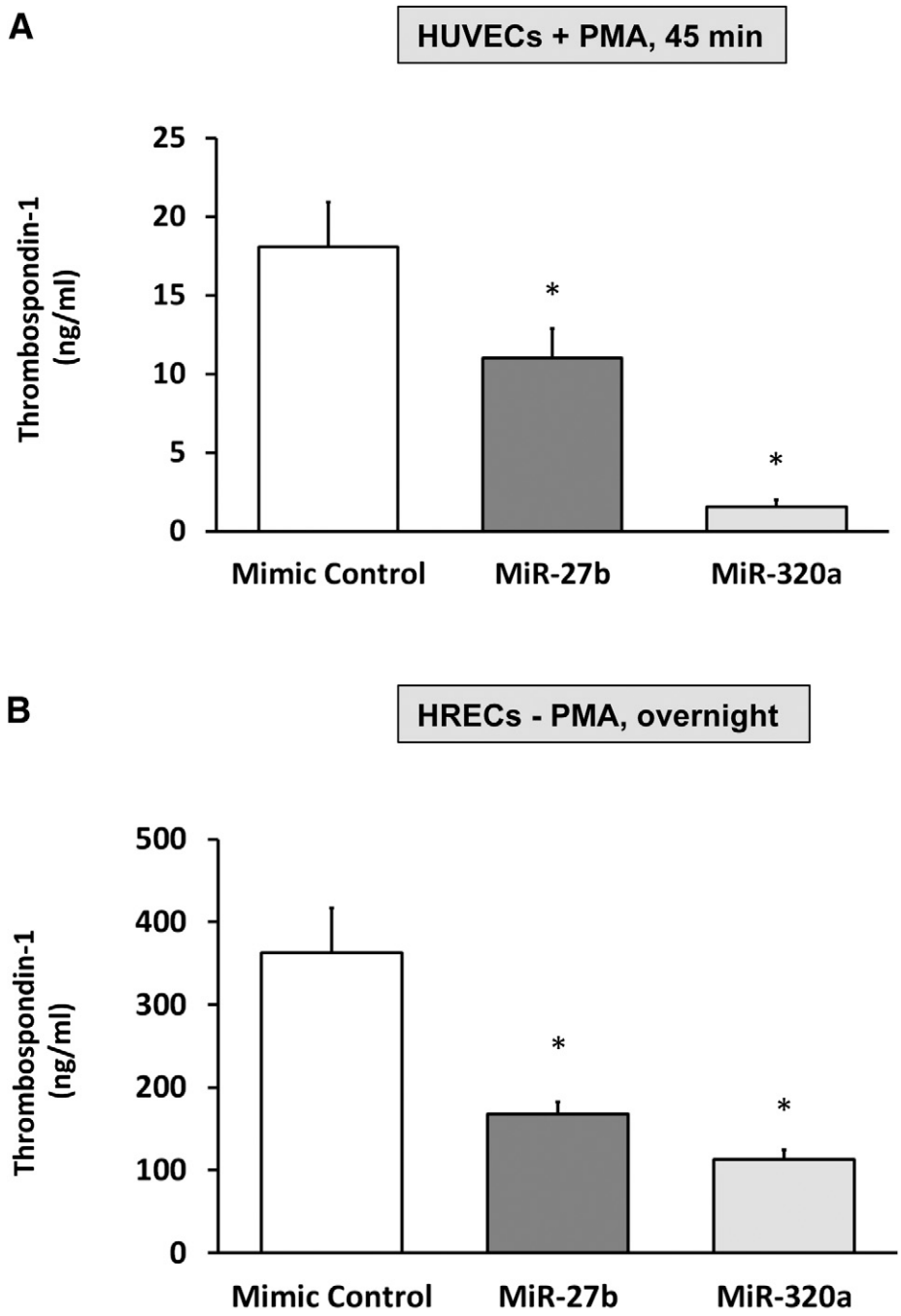

Figure 5—Validation of the proteomics findings by ELISA. Reduced secretion of TSP-1 in the endothelial secretome upon transfection with mimics of miR-27b and miR-320a. HUVECs after 45 min of PMA stimulation in serum-free medium (*A*) and HRECs after overnight serum deprivation in the presence of endothelial supplements (*B*). *$P < 0.05$.

including targets that would not have been anticipated based on current bioinformatics prediction models (11,16). To complement our clinical studies, we used a proteomics approach to identify putative protein targets of miR-27b and miR-320a in the secretome of ECs. HUVECs were stimulated with PMA to induce exocytosis of Weibel-Palade bodies, an endothelial cell–specific storage organelle, allowing for protein analysis by mass spectrometry. Among >650 proteins identified (Supplementary Table 3), only TSP-1 showed differential secretion from both miR-27b– and miR-320a–transfected ECs, relative to control transfected cells (Fig. 4*C* and *D*). The proteomics data were independently validated by ELISA (Fig. 5*A*). Similar results were obtained in HRECs after miR-27b or miR-320a overexpression (Fig. 5*B*). An alignment of the thrombospondin-1 gene (*THBS-1*) mRNA region with the sequence of miR-320a and miR-27b is shown in Fig. 6*A*. The vertical bars and bold characters indicate sequences of the miR-320a– and

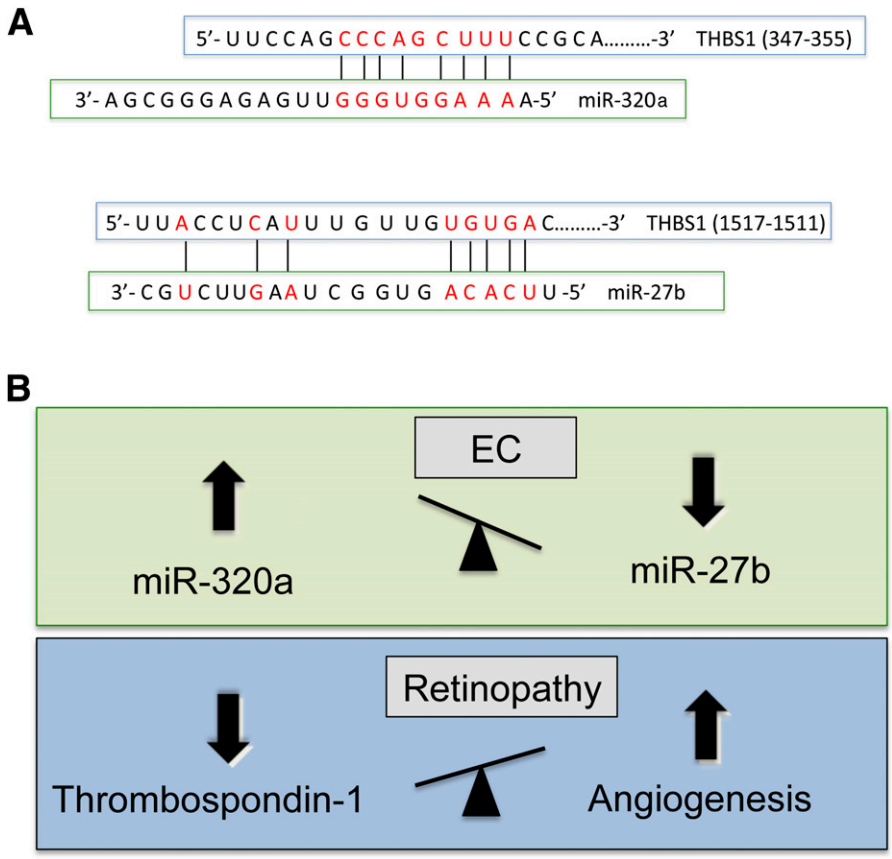

Figure 6—Angiogenic miRNAs. Alignment of THBS-1 mRNA region with miR-320a and miR-27b (*A*). Relative abundance of miR-320a and miR-27b in ECs and suppression of TSP-1 secretion as a shared molecular pathway (*B*). Circulating miRNA changes in patients with T1D and retinopathy, however, may represent markers of a milieu that is conducive to pathological angiogenesis rather than a local release from the retina.

miR-27b–binding site of the *THBS-1* target gene. As expected for direct miRNA targets, there was complementarity between the miR-27b seed-matching sequence and the 3′-untranslated region of the *THBS-1* target gene. According to one algorithm (miRWalk), TSP-1 was also predicted as a target for miR-320a. The putative seed-binding region, however, was within the coding region of the *THBS-1* gene. To further confirm the functionality of these predicted interactions, we fused the putative binding regions within the *THBS-1* target gene to a luciferase reporter vector. Coexpression of synthetic miR-27b, but not miR-320a, decreased *THBS-1* reporter activity (data not shown), confirming TSP-1 as a direct target of miR-27b (17) and an indirect target of miR-320a (Fig. 6*B*).

DISCUSSION

Using data from two independent prospective cohorts, we identified miR-27b and miR-320a as potential biomarkers for new-onset retinopathy or progression of retinopathy in patients with T1D. Both miR-27 and miR-320a have previously associated with metabolic syndrome and type 2 diabetes (18) and have been implicated in angiogenesis, providing a mechanistic underpinning for the observed association with diabetic retinopathy in the DIRECT cohort (9).

Retinopathy in T1D

Retinopathy remains the most frequent and most feared complication of T1D (19). It is associated with elevated risks of other diabetes complications, notably, nephropathy and cardiovascular disease (20). Although acknowledged as a vascular phenomenon, the only intervention proven to date to reduce onset or progression of retinopathy is tight glycemic control. This is difficult to achieve and is associated with elevated risks of hypoglycemic episodes. Significant numbers of individuals with T1D continue to progress to severe, possibly sight-threatening disease even in the presence of good glycemic control. There is therefore a need to discover novel biomarkers that identify individuals at high risk of progressive retinopathy and targets for therapeutic intervention.

miRNAs in T1D

miRNAs may offer distinct advantages over other biomarkers (8): Unlike messenger RNAs, miRNAs are stable in blood. As nucleic acids, miRNAs can be measured by

quantitative PCR methodology allowing the multiplexing of several miRNAs in a single experiment. Thus far, the role of miRNAs in diabetic retinopathy progression has been assessed in small animal models (21–26). Moreover, an miRNA-dependent cross talk between HIF1α and VEGF was reported in the diabetic retina (27). In this study, we show that miR-320a and miR-27b are associated with new-onset retinopathy or progression of retinopathy in patients with T1D. These findings were unaltered by excluding participants with incident persistent or intermittent microalbuminuria at any time during the follow-up.

Mechanistic Links to Angiogenesis

Besides its potential prognostic and diagnostic value, miRNAs may participate in an unexplored mechanism contributing to retinopathy in patients with T1D. Several miRNAs can target the same effector. Diverse miRNAs can also act cooperatively or redundantly to regulate the effectors of the same biological process. miR-320a regulates glycolysis and represses angiogenic factors, including Flk1, VEGFc, insulin-like growth factor 1, insulin-like growth factor 1 receptor, and fibroblast growth factor (28,29). miR-320a has also been implicated in tumor angiogenesis by silencing NRP1 (30). miR-27b is thought to promote angiogenesis by targeting antiangiogenic genes (31), including the transmembrane protein SEMA6A. The miR-23/-27/-24 gene clusters are enriched in ECs and highly vascularized tissues (32). miR-27b orchestrates endothelial tip cell formation (33,34). By analyzing protein targets of miR-27b and miR-320a in ECs, we obtained a more comprehensive depiction of the interactions and regulatory feedback loops between angiogenic proteins and our candidate miRNAs.

Proteomics Approach for miRNA Target Identification

The "targetome" of most miRNAs remains an unexplored aspect of current biology. Currently, the available miRNA target prediction tools are based on an incomplete understanding of miRNA target recognition and miRNA efficacy. Bioinformatic methodologies reveal numerous putative targets, but only one of five of the in silico predictions is correct, and experimental confirmation is essential. Proteomics methods can be useful for identifying miRNA targets at the protein level in addition to the use of bioinformatics prediction algorithms. We have pursued a proteomics approach to compare the effects of miR-27b and miR-320a on the secretome of ECs (10). TSP-1 was returned as a common target of both miR-27b and miR-320a (35). TSP-1 is an extracellular matrix protein, which inhibits EC proliferation, migration, and angiogenesis (36). Its antiangiogenic effect is mediated through an interaction with VEGF, specifically, via inhibition of VEGF receptor-2 activation through engaging its receptor CD47 (37). This has further been supported in vivo, specifically, in the eye: depletion of TSP-1 resulted in corneal neovascularization in mice (38). Of particular significance to diabetic retinopathy, a biphasic response of TSP-1 mediated through VEGF occurred in microvascular cells in the ischemic retina (39). This response tightly regulates VEGF and therefore indicates a potential negative feedback mechanism of VEGF-induced angiogenesis through TSP-1 (39). By now, several studies have implicated TSP-1 in pathological angiogenesis in the retina (40–42). TSP-1 has been shown to inhibit neovascularization in diabetic mice (43). Moreover, miR-27b rescued impaired angiogenesis via TSP-1 suppression (17). Our findings confirm that miR-27b directly suppresses reporter activity for TSP-1. In contrast, miR-320a has an indirect effect on TSP-1 secretion.

Strengths and Limitations of the Study

Our study was prospective and, hence, measured miRNA levels before occurrence of the disease outcome. Using a nested case-control approach, we identified 155 participants with retinopathy incidence/progression among DIRECT trial participants (overall n = 3,326) and compared miRNA profiles with those of matched control subjects. Associations were independent of established risk factors for diabetic retinopathy, including age, sex, HbA_{1c}, diabetes duration, and blood pressure, and were further underpinned by our biologically plausible finding from the proteomics analysis that both miRNAs target TSP-1. Still, whether miR-27b and miR-320a are causally involved in diabetes retinopathy or a marker of this disease remains to be clarified. The identified miRNAs are not retina specific. The changes in miR-27b and miR-320a may reflect a systemic predisposition for pathological angiogenesis. The cause for the differential regulation of circulating levels of miR-27b and miR-320a is currently unclear. For many biomarkers, the cellular origin remains uncertain. For example, both ECs as well as platelets secrete TSP-1. Measuring its circulating levels does not reveal how much of TSP-1 is endothelial or platelet derived. The same limitation applies to miRNAs that are not tissue specific and detected in the circulation. Both miR-320a and miR-27b are also present in platelets (6). The opposing directionality of the association of miR-27b and miR-320a with diabetic retinopathy could hint to a different cellular origin of these two circulating miRNAs; i.e., miR-320a is secreted at much higher levels from ECs than miR-27b. Further studies are required to provide an in-depth understanding of their cellular origin and to test the diagnostic or therapeutic potential of these two circulating miRNAs in diabetic retinopathy. We measured miRNA levels only at baseline and, hence, could not assess or take into account within-person variability of the miRNAs over time. Finally, model selection and parameter estimation were performed on the same data set without adjustment, which may lead to an overestimation of the strength of association obtained and underestimation of confidence limits.

Conclusions

Understanding how circulating miRNAs could be harnessed for assessing the risk of retinopathy in T1D is an essential area of research. Our data in the DIRECT trials

show that miR-320a and miR-27b are associated with new onset of retinopathy and progression of retinopathy. Besides identifying circulating miRNAs associated with retinopathy, we also interrogated the targets of miR-27b and miR-320a in ECs using a proteomics approach. Taken together, the findings of our study identify miRNA biomarkers for retinopathy in two independent cohorts. These findings await confirmation in larger studies, but our two lead miRNAs may have clinical utility given their established links to angiogenesis, including the translational control of TSP-1 by miR-27b and its reduced endothelial secretion by miR-320a.

Acknowledgments. The authors thank Raimund Pechlaner, Department of Neurology, Medical University of Innsbruck, and Philipp Skroblin, Cardiovascular Division, King's College London, for help with preparing the manuscript.

Funding. A.Z. is an Intermediate Fellow of the British Heart Foundation (FS/13/18/30207). P.W. is an Erwin Schrödinger Fellow in Epidemiology sponsored by the Austrian Science Fund. M.M. is a Senior Fellow of the British Heart Foundation (FS/13/02/29892). This work was supported in part by JDRF (17-2011-658), Diabetes UK (12/0004530), the Fondation Leducq (MicroRNA-based Therapeutic Strategies in Vascular Disease [MIRVAD] [13 CVD 02]), and the National Institute of Health Research Biomedical Research Center based at Guy's and St Thomas' National Health Service Foundation Trust and King's College London in partnership with King's College Hospital.

Duality of Interest. The DIRECT trial was jointly funded by AstraZeneca and Takeda. King's College London has filed patent applications on miRNA biomarkers. No other potential conflicts of interest relevant to this article were reported.

Author Contributions. A.Z., S.B., and X.Y. performed the experiments. A.Z., P.W., N.C., and M.M. wrote the manuscript. P.W., S.R.L., S.K., and N.C. analyzed data. R.K., N.C., and M.M. conceived and designed the experiments. P.R. provided the serum samples. M.M. is the guarantor of this work and, as such, had full access to all the data in the study and takes responsibility for the integrity of the data and the accuracy of the data analysis.

References

1. Zampetaki A, Mayr M. MicroRNAs in vascular and metabolic disease. Circ Res 2012;110:508–522
2. van Rooij E, Olson EN. MicroRNA therapeutics for cardiovascular disease: opportunities and obstacles. Nat Rev Drug Discov 2012;11:860–872
3. Kantharidis P, Wang B, Carew RM, Lan HY. Diabetes complications: the microRNA perspective. Diabetes 2011;60:1832–1837
4. Zampetaki A, Kiechl S, Drozdov I, et al. Plasma microRNA profiling reveals loss of endothelial miR-126 and other microRNAs in type 2 diabetes. Circ Res 2010;107:810–817
5. Zampetaki A, Willeit P, Tilling L, et al. Prospective study on circulating MicroRNAs and risk of myocardial infarction. J Am Coll Cardiol 2012;60:290–299
6. Willeit P, Zampetaki A, Dudek K, et al. Circulating microRNAs as novel biomarkers for platelet activation. Circ Res 2013;112:595–600
7. Zampetaki A, Willeit P, Drozdov I, Kiechl S, Mayr M. Profiling of circulating microRNAs: from single biomarkers to re-wired networks. Cardiovasc Res 2012;93:555–562
8. Mayr M, Zampetaki A, Willeit P, Willeit J, Kiechl S. MicroRNAs within the continuum of postgenomics biomarker discovery. Arterioscler Thromb Vasc Biol 2013;33:206–214
9. Chaturvedi N, Porta M, Klein R, et al.; DIRECT Programme Study Group. Effect of candesartan on prevention (DIRECT-Prevent 1) and progression (DIRECT-Protect 1) of retinopathy in type 1 diabetes: randomised, placebo-controlled trials. Lancet 2008;372:1394–1402
10. Yin X, Bern M, Xing Q, Ho J, Viner R, Mayr M. Glycoproteomic analysis of the secretome of human endothelial cells. Mol Cell Proteomics 2013;12:956–978
11. Abonnenc M, Nabeebaccus AA, Mayr U, et al. Extracellular matrix secretion by cardiac fibroblasts: role of microRNA-29b and microRNA-30c. Circ Res 2013;113:1138–1147
12. Higgins JP, Thompson SG. Quantifying heterogeneity in a meta-analysis. Stat Med 2002;21:1539–1558
13. Goeman JJ. L1 penalized estimation in the Cox proportional hazards model. Biom J 2010;52:70–84
14. Dhanabal M, Wu F, Alvarez E, et al. Recombinant semaphorin 6A-1 ectodomain inhibits in vivo growth factor and tumor cell line-induced angiogenesis. Cancer Biol Ther 2005;4:659–668
15. Miao HQ, Lee P, Lin H, Soker S, Klagsbrun M. Neuropilin-1 expression by tumor cells promotes tumor angiogenesis and progression. FASEB J 2000;14:2532–2539
16. Zampetaki A, Attia R, Mayr U, et al. Role of miR-195 in aortic aneurysmal disease. Circ Res 2014;115:857–866
17. Wang JM, Tao J, Chen DD, et al. MicroRNA miR-27b rescues bone marrow-derived angiogenic cell function and accelerates wound healing in type 2 diabetes mellitus. Arterioscler Thromb Vasc Biol 2014;34:99–109
18. Karolina DS, Tavintharan S, Armugam A, et al. Circulating miRNA profiles in patients with metabolic syndrome. J Clin Endocrinol Metab 2012;97:E2271–E2276
19. Diabetes Control and Complications Trial (DCCT)/Epidemiology of Diabetes Interventions and Complications (EDIC) Research Group, Lachin JM, White NH, Hainsworth DP, Sun W, Cleary PA, Nathan DM. Effect of intensive diabetes therapy on the progression of diabetic retinopathy in patients with type 1 diabetes: 18 years of follow-up in the DCCT/EDIC. Diabetes 2015;64:631–642
20. van Hecke MV, Dekker JM, Stehouwer CD, et al.; EURODIAB Prospective Complications Study. Diabetic retinopathy is associated with mortality and cardiovascular disease incidence: the EURODIAB Prospective Complications Study. Diabetes Care 2005;28:1383–1389
21. Kovacs B, Lumayag S, Cowan C, Xu S. MicroRNAs in early diabetic retinopathy in streptozotocin-induced diabetic rats. Invest Ophthalmol Vis Sci 2011;52:4402–4409
22. Feng B, Chen S, McArthur K, et al. miR-146a-mediated extracellular matrix protein production in chronic diabetes complications. Diabetes 2011;60:2975–2984
23. Silva VA, Polesskaya A, Sousa TA, et al. Expression and cellular localization of microRNA-29b and RAX, an activator of the RNA-dependent protein kinase (PKR), in the retina of streptozotocin-induced diabetic rats. Mol Vis 2011;17:2228–2240
24. McArthur K, Feng B, Wu Y, Chen S, Chakrabarti S. MicroRNA-200b regulates vascular endothelial growth factor-mediated alterations in diabetic retinopathy. Diabetes 2011;60:1314–1323
25. Murray AR, Chen Q, Takahashi Y, Zhou KK, Park K, Ma JX. MicroRNA-200b downregulates oxidation resistance 1 (Oxr1) expression in the retina of type 1 diabetes model. Invest Ophthalmol Vis Sci 2013;54:1689–1697
26. Bai Y, Bai X, Wang Z, Zhang X, Ruan C, Miao J. MicroRNA-126 inhibits ischemia-induced retinal neovascularization via regulating angiogenic growth factors. Exp Mol Pathol 2011;91:471–477
27. Ling S, Birnbaum Y, Nanhwan MK, Thomas B, Bajaj M, Ye Y. MicroRNA-dependent cross-talk between VEGF and HIF1α in the diabetic retina. Cell Signal 2013;25:2840–2847
28. Tang H, Lee M, Sharpe O, et al. Oxidative stress-responsive microRNA-320 regulates glycolysis in diverse biological systems. FASEB J 2012;26:4710–4721
29. Wang X, Huang W, Liu G, et al. Cardiomyocytes mediate anti-angiogenesis in type 2 diabetic rats through the exosomal transfer of miR-320 into endothelial cells. J Mol Cell Cardiol 2014;74:139–150
30. Wu YY, Chen YL, Jao YC, Hsieh IS, Chang KC, Hong TM. miR-320 regulates tumor angiogenesis driven by vascular endothelial cells in oral cancer by silencing neuropilin 1. Angiogenesis 2014;17:247–260
31. Kuehbacher A, Urbich C, Zeiher AM, Dimmeler S. Role of Dicer and Drosha for endothelial microRNA expression and angiogenesis. Circ Res 2007;101:59–68

32. Zhou Q, Gallagher R, Ufret-Vincenty R, Li X, Olson EN, Wang S. Regulation of angiogenesis and choroidal neovascularization by members of microRNA-23~27~24 clusters. Proc Natl Acad Sci U S A 2011;108: 8287–8292
33. Urbich C, Kaluza D, Frömel T, et al. MicroRNA-27a/b controls endothelial cell repulsion and angiogenesis by targeting semaphorin 6A. Blood 2012;119: 1607–1616
34. Biyashev D, Veliceasa D, Topczewski J, et al. miR-27b controls venous specification and tip cell fate. Blood 2012;119:2679–2687
35. Stenina-Adognravi O. Thrombospondins: old players, new games. Curr Opin Lipidol 2013;24:401–409
36. Tolsma SS, Stack MS, Bouck N. Lumen formation and other angiogenic activities of cultured capillary endothelial cells are inhibited by thrombospondin-1. Microvasc Res 1997;54:13–26
37. Kaur S, Martin-Manso G, Pendrak ML, Garfield SH, Isenberg JS, Roberts DD. Thrombospondin-1 inhibits VEGF receptor-2 signaling by disrupting its association with CD47. J Biol Chem 2010;285:38923–38932
38. Cursiefen C, Masli S, Ng TF, et al. Roles of thrombospondin-1 and -2 in regulating corneal and iris angiogenesis. Invest Ophthalmol Vis Sci 2004;45: 1117–1124
39. Suzuma K, Takagi H, Otani A, Oh H, Honda Y. Expression of thrombospondin-1 in ischemia-induced retinal neovascularization. Am J Pathol 1999;154:343–354
40. Kermorvant-Duchemin E, Sennlaub F, Sirinyan M, et al. Trans-arachidonic acids generated during nitrative stress induce a thrombospondin-1-dependent microvascular degeneration. Nat Med 2005;11:1339–1345
41. Choi J, Lin A, Shrier E, Lau LF, Grant MB, Chaqour B. Degradome products of the matricellular protein CCN1 as modulators of pathological angiogenesis in the retina. J Biol Chem 2013;288:23075–23089
42. Sorenson CM, Wang S, Gendron R, Paradis H, Sheibani N. Thrombospondin-1 deficiency exacerbates the pathogenesis of diabetic retinopathy. J Diabet Metabol S12:005 doi: 10.4172/2155-6156.S12-005
43. Ii M, Takenaka H, Asai J, et al. Endothelial progenitor thrombospondin-1 mediates diabetes-induced delay in reendothelialization following arterial injury. Circ Res 2006;98:697–704
44. Levey AS, Stevens LA, Schmid CH, et al.; CKD-EPI (Chronic Kidney Disease Epidemiology Collaboration). A new equation to estimate glomerular filtration rate. Ann Intern Med 2009;150:604–612
45. Levey AS, Coresh J, Greene T, et al.; Chronic Kidney Disease Epidemiology Collaboration. Expressing the Modification of Diet in Renal Disease Study equation for estimating glomerular filtration rate with standardized serum creatinine values. Clin Chem 2007;53:766–772
46. Williams KV, Erbey JR, Becker D, Arslanian S, Orchard TJ. Can clinical factors estimate insulin resistance in type 1 diabetes? Diabetes 2000;49: 626–632